ELSEVIER

Physica E 2 (1998) 578–582

PHYSICA E

Hot carrier relaxation in InAs/GaAs quantum dots

R. Heitz[a,b,*], M. Veit[b], A. Kalburge[a], Q. Xie[a], M. Grundmann[b], P. Chen[a], N.N. Ledentsov[b], A. Hoffmann[b], A. Madhukar[a], D. Bimberg[b], V.M. Ustinov[c], P.S. Kop'ev[c], Zh.I. Alferov[c]

[a] *Photonic Materials and Devices Laboratory, University of Southern California, Los Angeles, California 90089-0241, USA*
[b] *Institut für Festkörperphysik, Technische Universität Berlin, 10623 Berlin, Germany*
[c] *A.F. Ioffe Physical-Technical Institute, 194021, St. Petersburg, Russian Federation*

Abstract

Excited states and energy relaxation processes are studied for self-organized InAs/GaAs quantum dots (QDs). Photoluminescence excitation (PLE) spectra show sample-dependent either multi-LO-phonon resonances or excited state transitions, revealing the dominant carrier relaxation mechanism or the size-dependent excited state splitting of the QDs, respectively. Time-resolved photoluminescence results indicate sample-dependent non-radiative recombination, suggesting a model for the observed PLE behavior, analogous to hot carrier relaxation in higher-dimensional systems. Carrier relaxation in the self-organized InAs/GaAs QDs proceeds by multi-LO-phonon scattering on a 40 ps time scale, which is short compared to radiative (>500 ps) and non-radiative (>100 ps) recombination times, accounting for the absence of a phonon bottleneck effect in PL spectra. However, carrier relaxation might effect the stimulated emission region.

Keywords: Quantum dots; Carrier relaxation; Time-resolved photoluminescence; Excited states

1. Introduction

The spontaneous formation of coherent semiconductor islands in highly strained epitaxy has attracted interest as nature's way of generating nm-scale quantum dots (QDs). The defect-free coherent nature of the islands [1] led to the demonstration of QD-based injection lasers [2,3]. However, hot carrier relaxation processes, crucial for device performance, are not well understood as yet [4–13].

The discrete atomic-like energy spectrum of QDs constrains carrier relaxation due to inelastic phonon scattering [4,5]. Indeed, inter-level scattering times of the order of some 10 ps or longer have been inferred from time-resolved PL (TRPL) results [8,10] or rate equation models [11]. The long relaxation-limited lifetime of the excited states makes the QDs sensitive to competing non-radiative recombination processes, which ultimately might suppress ground state PL, the so-called phonon bottleneck effect [4]. PL excitation (PLE) spectra of InAs QDs are reported to show excited state transitions [12,13] or phonon resonances

* Corresponding author. Tel.: + 1 213 740 4330; fax: + 1 213 740 4333; e-mail: robert@photonics.usc.edu.

1386-9477/98/$19.00
PII: S1386-9477(98)00118-0

attributed to the carrier relaxation dynamics [6–8] or resonance enhancement [9].

In this paper we report on PLE and TRPL studies of self-organized InAs/GaAs QDs. Two types of samples, distinguished by their respective characteristic PLE and TRPL behavior, are compared, yielding insight into the carrier relaxation processes and the relaxation and recombination dynamics.

2. Samples and experimental setup

Two types of InAs/GaAs QD samples were grown by solid source MBE on GaAs (0 0 1) substrate. For type A samples multiple InAs layers (each 1.74 ML) were deposited at 500°C and separated and capped with GaAs grown at 400°C using migration enhanced epitaxy as described in Refs. [12,14]. The 20 or 36 ML spacers result in vertical ordering (>95%) of the InAs islands [14]. For type B samples a single InAs layer (12 Å) was deposited and capped with 10 nm GaAs at 480°C as described in Refs. [2,6].

PLE was measured in a continuous-flow He-cryostat using a tungsten lamp dispersed by a 0.27 m double-grating monochromator as a tunable light source. TRPL was measured in superfluid He with a tunable Ti-Sapphire laser providing 150 fs pulses and a subtractive double-grating monochromator in combination with an infrared-enhanced streak camera. Time constants down to 5 ps could be resolved taking into account the system response function.

3. Experimental results

Fig. 1a shows PL (inset) and PLE spectra for a type A sample with 5 InAs layers and 36 ML spacers. The excess excitation energy $\Delta E = E_{\mathrm{exc}} - E_{\mathrm{det}}$ of the dominating PLE resonance (FWHM = 25 meV) decreases from 96 to 70 meV with decreasing detection energy, which we attribute to the decreasing excited state splitting with increasing QD size. High-density PL spectra reveal the first excited state transition 79 meV above the ground-state transition (not shown here) in agreement with

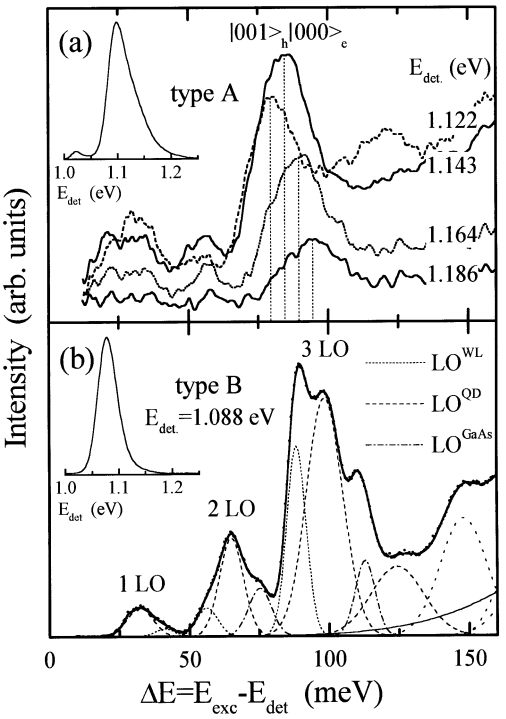

Fig. 1. PLE spectra for a type A sample with 5 QD layers and 36 ML spacer (a) and a single-layer type B sample (b). The insets show the respective PL spectra for GaAs barrier excitation.

the PLE results. The experimental excited state splitting and its size dependence are in reasonable agreement with numerical results for pyramidal InAs QDs [15] supporting the assignment of the PLE resonance to the transition between the $|0\,0\,1\rangle_h$ excited hole state and the $|0\,0\,0\rangle_e$ electron ground-state. Spectra excited with a tunable Ti-Sapphire laser reveal Raman scattering in the energy region below 40 meV.

The excited state transition is not resolved in the PLE spectra of the type B sample. Fig. 1b shows the PL spectrum (inset) and the PLE behavior recorded at the PL maximum. Instead, starting at the detection energy a regularly spaced series of line groups evolves with the third one centered near 100 meV dominating the spectrum. The energy spacing of about 32 meV suggests a phononic origin of these resonances. A threefold substructure is resolved for the 60 and 100 meV line groups. A line

shape fit with multiple Gaussians (full line in Fig. 1b) shows that the various excitation resonances with FWHMs between 7 and 14 meV can be explained as multi-phonon replicas with phonon energies of (29.6 ± 0.5), (32.6 ± 0.5) and (37.6 ± 0.5) meV. Multiples but no combinations of the phonon modes are resolved. The excess energy of the PLE resonances is independent of the detection energy although the relative intensity of the lines varies slightly. PL excited selectively with high-density at 1064 nm showed GaAs Raman scattering to contribute to the 1 LO peak [6]. The characteristic phonon energies let us assign the three observed phonon modes to the InAs WL, the InAs QDs and the strained GaAs barrier near the QDs [8]. The large FWHM of the PLE resonances (>7 meV) might result from weakened k-selection rules and/or higher-order processes involving LA phonons [5]. The phonon replica are *local* probes of the strain in and around the overgrown InAs islands supporting the *coherent* nature of the optically active QDs.

The different PLE behavior observed for type A and B samples (Fig. 1) is determined by the carrier relaxation and recombination dynamics. Fig. 2 shows PL transients recorded for excitation densities at which the QDs are initially completely saturated. The transients show an almost constant intensity as long as PL from higher energy states is observed. Relaxation of carriers from higher energy states keeps the ground-state population constant. The transients in Fig. 2a and b show that the carrier density in the QDs decay much slower for the type A sample, leading to resolved saturation for the $|0\,0\,1\rangle$ and $|0\,0\,2\rangle$ excited hole states which is not observed for the type B sample. At a given time only PL from the highest populated level will decay and the time constant is given by the sum of the recombination rates of all carriers in the QD. Multi-exponential fits yield for the type A (B) sample decay times of 480 (95) ps for the first excited $|0\,0\,1\rangle$ state, 180 (42) ps for the second excited $|0\,0\,2\rangle$ state, and 15 (<5) ps for the WL. Master equations for micro-states (MEM) provide a correct description of the QD PL dynamics under saturation conditions [16]. A MEM fit for the type A sample determines the radiative lifetime of the $|0\,0\,1\rangle$ excited hole state to 1550 ps in good agreement with the 'forbidden' character of the $|0\,0\,1\rangle_h|0\,0\,0\rangle_e$ transition [15]. The faster decay of the excited state PL in the type B sample indicates an extrinsic non-radiative recombination channel with time constants of about 120 and 55 ps for the $|0\,0\,1\rangle$ and $|0\,0\,2\rangle$ hole states, respectively. Since the PLE results show the optically active InAs islands to be coherent, we propose energy transfer to deep defects in the vicinity of the InAs islands. The decreasing hole localization in the excited states and, in particular, in the WL, accounts for the increasing non-radiative recombination probability.

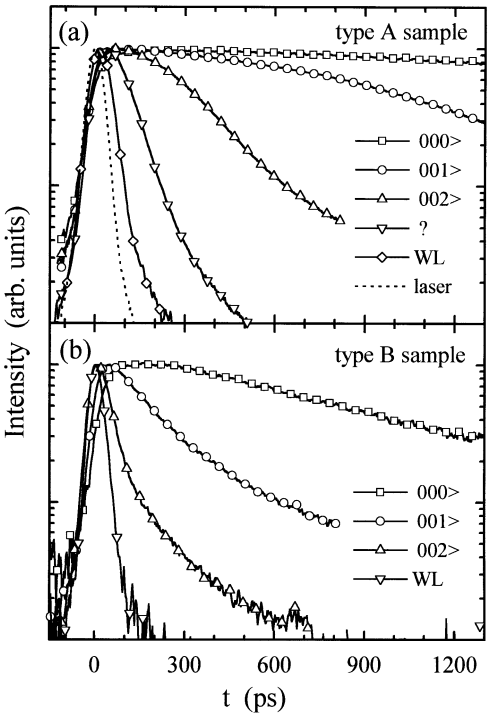

Fig. 2. High density PL transients of the ground and excited QD transition peaks for a 5 QD-layer type A sample with 20 ML spacers (a) and a type B sample (b).

In higher-dimensional systems multi-LO-phonon resonances in PLE spectra are known to result from hot carrier relaxation when competing non-radiative recombination allows only the most efficient relaxation processes to populate the luminescent state [17]. For QDs having a discrete

density of states the inhomogeneous broadening of the ensemble replaces the spatial dispersion in higher-dimensional systems. The non-radiative recombination in the type B sample allows only QDs with rapid carrier relaxation to contribute to the PLE signal. Fig. 1b thus shows a resonance condition ($\Delta E = n \times \hbar\omega_{LO}$) demonstrating that carrier relaxation in small self-assembled QDs proceeds via inelastic phonon scattering needing multiple LO phonons to bridge the energy gap between the discrete states. However, the coupling to various LO modes and the FWHM of the multi-LO resonance establish wide energy windows for efficient carrier relaxation. On the contrary for the type A sample, the low non-radiative recombination rate demonstrated in the TRPL experiments (Fig. 2) also allows out-of-resonance QDs to contribute to the PLE signal, which then follows the absorption spectrum. In fact, the excited state PLE resonance peaks for $\Delta E \approx 83$ meV, corresponding to a minimum in the multi-LO-phonon relaxation probability. The results demonstrate the extrinsic nature of the competing recombination channel.

The large FWHM (25 meV) of the excited state PLE resonance in the type A sample is attributed to the inhomogeneous excited state broadening for a fixed ground state transition energy resulting from shape variations of the islands. PLE results suggest that for single-layer samples the inhomogeneous excited state broadening is larger and that vertical self-organization of the islands improves the shape uniformity [13]. In the type B sample the average excited state splitting is also in the 90 meV region accounting for the dominance of the 3 LO resonances in the PLE spectra.

The carrier relaxation rate and ground-state lifetime are obtained from low excitation density transients, which are well fitted by two exponentials describing the PL rise and decay, respectively. The ground-state decay time for type A samples ranges between 500 and 800 ps and is practically independent of the detection energy and therefore the QD size, Fig. 3a. Theory predicts the inter-band oscillator strength to be independent of the QD size in the strong confinement regime [18], which is given for the small InAs QDs. For the type B sample the ground-state decay time is (1070 ± 100) ps for large QDs and decreases to 500 ps for smaller ones. The

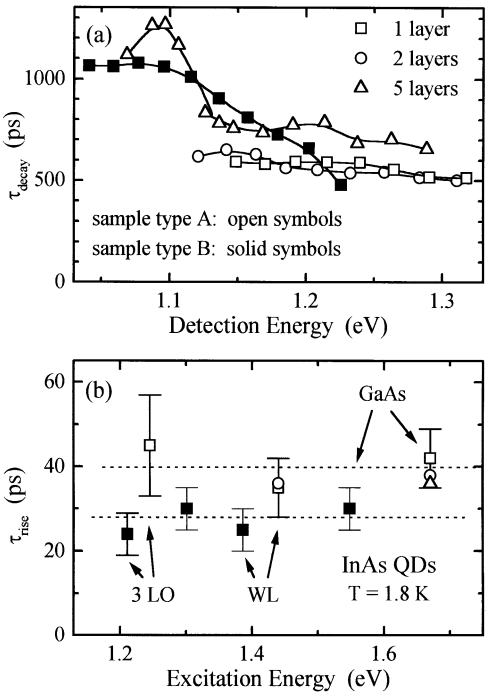

Fig. 3. PL decay (a) and rise (b) times derived from two-exponential fits of low excitation density PL transients for type A samples (open symbols) and the type B sample (solid squares).

non-radiative recombination observed for excited states might influence the ground-state transition of the smaller QDs. The present results are in good agreement with previously reported decay times [2,19] and suggest that the decay time might depend on the QD shape.

The PL rise time is independent of the chosen excitation energy/process, being (40 ± 5) and (28 ± 5) ps for type A and B samples, respectively (Fig. 3b). The same transients are observed exciting non-resonantly the GaAs barrier or the WL or resonantly the $|0\,0\,1\rangle_h|0\,0\,0\rangle_e$ excited state transition, indicating the $|0\,0\,1\rangle$ hole state to be the bottleneck in the capture and relaxation cascade. Taking into account the non-radiative recombination observed for the type B sample, the multi-LO-phonon relaxation time is (40 ± 5) ps for both sample types. The majority of the QDs in the investigated samples have an excited state splitting in the 3 LO range (Figs. 1 and 2). For larger QDs with an

excited state splitting in resonance with 2 or 1 LO processes, inelastic phonon scattering is expected to be more efficient. Finally, the temperature dependence of the PLE spectra suggests thermal evaporation of carriers from excited QD states to cause the PL intensity decrease around 80 K generally observed for non-resonant excitation [13].

4. Conclusion

The observation of multi-LO-phonon resonances in the PLE spectra of small InAs/GaAs QDs unambiguously proves inelastic phonon scattering to be the dominant intra-dot relaxation process. The $|0\,0\,1\rangle$ hole state is found to be the relaxation bottleneck emphasizing the crucial role of a slowed-down carrier relaxation in small QDs. Carrier cooling is about two orders of magnitude slower than in higher-dimensional systems but still over an order of magnitude faster than radiative recombination explaining the apparent lack of a phonon bottleneck effect in PL experiments. Carrier relaxation is found to limit the PL yield at temperatures above 80 K and might lead to a bottleneck effect in the stimulated emission regime, limiting the high-frequency behavior of QD injection lasers and favouring lasing on excited state transitions.

Acknowledgements

Parts of this work were supported by the US Air Force Office of Scientific Research, the US Office of Naval Research, and the Deutsche Forschungsgemeinschaft in the framework of Sondernforschungsbereich 296.

References

[1] S. Guha et al., Appl. Phys. Lett. 57 (1990) 2110.
[2] N.N. Ledentsov et al., Microelectr. J. 26 (1995) 871.
[3] Q. Xie et al., IEEE Photon. Technol. Lett. 8 (1996) 965.
[4] H. Benisty et al., Phys. Rev. B 44 (1991) 10945.
[5] T. Inoshita, H. Sakaki, Phys. Rev. B 46 (1992) 7260.
[6] R. Heitz et al., Appl. Phys. Lett. 68 (1996) 361.
[7] M.J. Steer et al., Phys. Rev. B 54 (1997) 17738.
[8] R. Heitz et al., to be published.
[9] K.H. Schmidt et al., Phys. Rev. B 54 (1996) 11346.
[10] B. Ohnesorge et al., Phys. Rev. B 54 (1996) 11532.
[11] K. Mukai et al., Appl. Phys. Lett. 68 (1996) 3013.
[12] Q. Xie et al., J. Crystal Growth 150 (1995) 357.
[13] R. Heitz et al., In: M. Scheffler, R. Zimmermann (Eds.), Proc. 23rd Int. Conf. on the Physics of Semiconductors, Berlin, Germany, 1996, World Scientific, Singapore 1996, p. 1425.
[14] Q. Xie et al., Phys. Rev. Lett. 75 (1995) 2542.
[15] M. Grundmann et al., Phys. Rev. B 52 (1995) 11969.
[16] M. Grundmann, D. Bimberg, Phys. Rev. B 55 (1997) 9740.
[17] S.A. Permogorov, Phys. Stat. Sol. B 68 (1975) 9.
[18] E. Hanamura, Phys. Rev. B 37 (1988) 1273.
[19] G. Wang et al., Appl. Phys. Lett. 64 (1994) 2815.